

Two-Dimensional Diffraction by Half-Planes and Wide Slits Near Radiating Apertures

Hong D. Cheung and Edward V. Jull, *Life Fellow, IEEE*

Abstract—With the complex source-point method used to produce the basis elements of an array of linearly and directionally equispaced two-dimensional (2-D) beams, the fields of any aperture distribution at any range to any degree of accuracy can be obtained. For efficiency a limited number of significant beams and beam directions is required. Approximately twice as many beams as the aperture width in wavelengths, with all beam directions normal to the aperture, is found to be sufficient here for simple uniform and cosinusoidal distributions in apertures of moderate size at ranges outside the evanescent field zone of the aperture. Now the exact solution for the far field of a line source, or here a beam source in the presence of a conducting half-plane, is used as our basis element to give the solution for antenna pattern diffraction by a local half-plane. Antenna pattern diffraction by an aperture near a wide slit is presented as simply a superposition of the solutions for two coplanar half-planes with separated parallel edges. Antenna pattern distortion by various other local obstacles can be obtained similarly.

Index Terms—Apertures, electromagnetic diffractions, Gaussian beams.

I. INTRODUCTION

ADIOWAVE blockage by buildings is a problem common to mobile radio and cellular telephone systems in high-density urban areas. If the transmitting antenna has an omnidirectional pattern or the source is distant, the scattered field can be calculated by the techniques of high frequency diffraction theory such as the geometrical theory of diffraction. If the antenna beam is directive and the source is local, the omnidirectional source solution can be converted to a beam-source solution by the complex source point (CSP) method. Antenna patterns with sidelobes can be synthesized from arrays of beams, each with appropriate amplitude, phase, and direction. Their individual scattering from apertures and buildings may be calculated and the result summed for the total field. This paper begins by synthesizing antenna patterns from arrays of complex sources in two dimensions. Their far- and near-field patterns are then calculated. The scattering obstacles examined here are simple plane surfaces with edges, half-planes, and slits, but any structure for which a far-field omnidirectional source solution is available can be treated similarly.

A superposition of Gaussian beams is efficient for synthesizing the radiation fields of extended sources [1], [2]. This arrangement is based on that first proposed by D. Gabor for

the spectral decomposition of signals [3]. A two-dimensional (2-D) array of Gaussian beams, equispaced linearly and directionally, with each beam direction having a particular beamwidth and phase and both real and imaginary beam directions included, can represent the propagating and evanescent fields of any aperture distribution to any desired accuracy. For efficiency it is usually necessary to limit the number of beams and beam directions to those which contribute significantly to the total field in a particular application. This is the basis of the approach used here, except that the beams used are formed by the CSP method and so are only paraxially Gaussian.

It is well known that assigning a complex value to a source coordinate converts an omnidirectional point or line source into a beam that is paraxially Gaussian [4]–[6]. This source is a solution of the wave equation, whereas a Gaussian function is only an approximate solution. While the numerical difference between Gaussian beams and CSP beams is insignificant with many beams used and is essentially negligible in most situations, there is a very significant analytical advantage in using CSP beams in that they yield the possibility of using rigorous solutions for point or line source diffraction by canonical structures. This advantage is exploited here. The exact solution for the far of a line source parallel and near to a perfectly conducting half-plane is used as the basis function solution in our array. The solution is expressed uniformly in terms of Fresnel integrals. The line source solutions are then converted to paraxially Gaussian beam solutions by the complex source coordinate substitution. The Fresnel integral arguments become complex but these integrals are complimentary error functions with complex arguments, which can be computed with a standard subroutine. This approach was used for diffraction of a single beam by a local half-plane [7]. Now it is applied to an array of such beams constituting an antenna aperture distribution.

Of course, a simple half-plane solution is a canonical solution for other structures. Two coplanar half-planes with separated parallel edges form a slit. The total diffracted field will be the field scattered from the two half-planes in isolation plus their interaction scattered fields. These can be calculated by the geometrical theory of diffraction. Diffraction of a single beam by a slit was obtained this way [7] and here the same approach is used for aperture antenna beam diffraction by the slit.

This paper begins by examining the number of beams which contribute significantly to the far and near radiation fields of apertures. Earlier studies using both aligned and tilted beams [1], [2] and further calculations are a guide to the conclusion

Manuscript received April 6, 1998; revised July 8, 1999.

The authors are with the Department of Electrical and Computer Engineering, University of British Columbia, Vancouver, BC, V6T 1Z4 Canada.

Publisher Item Identifier S 0018-926X(99)09945-7.

here that the arrangement with the minimum number of significant beams seems to be that in which all beams are aligned with their axes normal to the aperture and spaced a half wavelength apart. This holds provided the evanescent fields of the aperture are negligible; that is for ranges outside the aperture plane but still well within the Fresnel zone of the aperture. We also examine here the effect of using CSP instead of Gaussian beams and the effect of the aperture distribution on the required number of beams. Not surprisingly a symmetrical tapered distribution, such as a cosine-squared distribution, which resembles a Gaussian distribution, requires fewer beams to represent the pattern than a uniform distribution. It is, however, the arrangement of beams within the Gabor lattice which ensures that any accuracy desired is obtained for a particular aperture distribution and range from the scatterer. Here only half-planes and simple combinations thereof are the scatterers, but scattering by structures such as wedges and cylinders have been similarly treated.

II. SYNTHESIS OF ANTENNA PATTERNS

A. Gabor's Expansion

Two-dimensional antenna fields can be constructed from a superposition of Gaussian beams. This is a so-called "Gabor series" [2] representation of the aperture field. Thus

$$E_z(x, 0) = \sum_{m=-\infty}^{\infty} \sum_{n=-\infty}^{\infty} A_{m,n} w(x - mL) e^{-j2n\pi x/L} \quad (1)$$

Here $E_z(x, 0)$ is the aperture electric field distribution in $y = 0$, $w(x)$ is a finite energy window function which is a Gaussian function in the Gabor series representation, and L is the spacing between Gaussian beams along x axis. Although proposed by Gabor in 1946, use of this nonorthogonal representation has been limited by difficulties in computing the series coefficients $A_{m,n}$. These difficulties have been partly removed [3], [9] and the coefficient $A_{m,n}$ may be obtained by convolving the desired aperture distribution with a biorthogonal function as described in [2]. The field in $y > 0$ can be written as

$$E_z(x, y) = \sum_{m=-\infty}^{\infty} \sum_{n=-\infty}^{\infty} A_{m,n} B_{m,n}(x, y) \quad (2)$$

where $B_{m,n}(x, y)$ are the elementary beam fields of the source functions. These are Gaussian functions in a Gabor series representation, but CSP beams here.

B. Complex Beam Sources

Assigning complex values to the coordinates of radiating point or line sources produce beams, which are paraxially Gaussian [4]–[6]. The far field of a 2-D electric line source is

$$E_z^i \approx \frac{e^{-jkR_s}}{\sqrt{kR_s}}, \quad kR_s \gg 1 \quad (3)$$

where $k = 2\pi/\lambda$ is the free-space wavenumber and

$$R_s = \sqrt{r^2 + r_s^2 - 2rr_s \cos(\theta - \theta_s)} \quad (4)$$

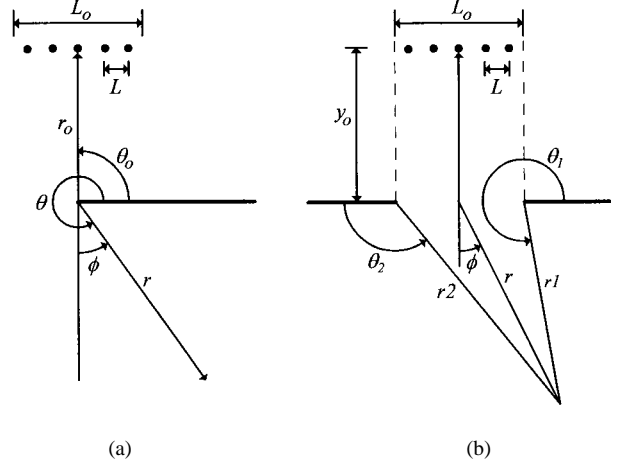


Fig. 1. (a) Geometry of an array of complex source beams in diffraction by a conducting half-plane. (b) Geometry of an array of complex source beams for diffraction at a slit.

is the distance from the complex source coordinates (r_s, θ_s) to the field point at (r, θ) . In [8, eqs. (3), (4)] relate (r_s, θ_s) to the real source coordinates (r_o, θ_o) for beam directivity and direction parameters (b, β) and [8, eq. (5)] gives the half-power beamwidth. Thus

$$E_z^i = \frac{e^{-jk(r-r_o \cos(\theta-\theta_o))}}{\sqrt{kr}} e^{kb \cos(\theta-\beta)}; \quad r \gg r_o \quad (5)$$

which represents an omnidirectional cylindrical wave modulated by a beam pattern $e^{kb \cos(\theta-\beta)}$ with its maximum in the direction $\theta = \beta$.

A single CSP generates a real beam without radiation pattern sidelobes. More realistic antenna radiation patterns having sidelobes require radiation from more than one source. It has already been shown that antenna patterns with sidelobes can be synthesized from arrays of Gaussian beams [1], [2] and that this representation applies to both near and far radiation patterns of the apertures. Here such arrays of complex sources located at complex locations ($x = mL$) are controlled by beam parameters $b_n = [L \cos(\beta_n - 3\pi/2)]^2/\lambda$, which defines beam directivity with λ the wavelength and $\beta_n = 3\pi/2 + \sin^{-1}(n\lambda/L)$, is the direction of the elementary beam axis off the line of the array. The radiating fields arise from beams with real direction angles (β_n real), and the beams with complex beam directions (β_n complex) contribute to the reactive fields of the aperture. Thus, the total field in $y > 0$ can be written as

$$E_z = \sum_{m=-M}^M \sum_{n=-N}^N A_{m,n} E_{z[m,n]}^i. \quad (6)$$

Here, $E_{z[m,n]}^i$ is given by (3) with $R_{s[m,n]}$ replacing R_s and

$$\begin{aligned} R_{s[m,n]} &= \sqrt{r^2 + r_{s[m,n]}^2 - 2rr_{s[m,n]} \cos(\theta - \theta_{s[m,n]})} \\ r_{s[m,n]} &= \sqrt{r_{o[m]}^2 - 2jr_{o[m]}b_n \cos(\beta_n - \theta_{o[m]}) - b_n^2} \\ \theta_{s[m,n]} &= \cos^{-1} \left(\frac{r_{o[m]} \cos \theta_{o[m]} - jb_n \cos \beta_n}{r_{s[m,n]}} \right). \end{aligned} \quad (7)$$

C. Numerical Results

It has been shown [2] that a reasonable and possibly the best choice for accurate far-field radiation patterns is to select the separation between two source points $L = (N + \frac{1}{2})\lambda$ (N is the largest integer n for real β_n). To simplify our analysis we chose all spacings $L = \lambda/2$ and let $N = 0$ so that all beam directions are real and orthogonal to the line of the array. Then $b = L^2/\lambda$, $kb = \pi/2$ and each CSP half-power beamwidth is 77.6° [8, eq.(5)].

Far-field radiation patterns of in-phase cosine-squared and uniform distributions in apertures of widths $L_o = 2.5\lambda$ and 5λ are shown in Fig. 2(a), (b) and (c), (d), respectively. The solid curves in Fig. 2 are the total far-field calculated from complex sources located along the aperture plane with different weighting factors. The dotted curves result from using Gaussian beams. These results are compared with the reference patterns (dashed curves) calculated from the truncated Fourier transform of cosine-squared and uniform field distributions in an aperture of width L_o , with zero field assumed in the aperture plane outside the aperture.

It is apparent that more line sources need to be included in the beam series computation for a uniform distribution than for a cosine-squared distribution with the same aperture size. In accordance with earlier results [1], [2], the aperture width and the amplitude profile of the aperture field determine the number of line sources needed. For smaller apertures and for aperture distributions tapered toward the edge of the profile, fewer line sources are needed for the same accuracy. Diffraction by local obstacles is of course simpler to calculate if fewer sources represent the radiating aperture.

Fig. 2 shows negligible differences between beam array solutions and reference patterns over the main beam and, for the larger apertures, the first sidelobes of the pattern. As the aperture size increases more beams are used and both Gaussian and CSP beams accurately produce the reference pattern over increasing numbers of sidelobes. At angles far off the beam axis, however, larger discrepancies occur in both Gaussian beam and CSP solutions. The CSP beam yield values above the reference solution and Gaussian beam solutions as $\phi \rightarrow 90^\circ$ because they are only paraxially Gaussian and do not approach zero far off the beam axis. Consequently, for small apertures with wide angle sidelobes [as in Fig. 2(a)] the first sidelobe level is inaccurately predicted by this CSP beam solution. Previous numerical results for similarly small apertures but with wider beam spacing and more beams [2, figs. 12, 13] show Gaussian beam solutions also fail to accurately predict the reference pattern at large angles ϕ off the beam axis. Elementary beams which vanish as $\phi \rightarrow 90^\circ$ can accurately produce the reference pattern at large angles ϕ [2, figs. 12, 13], but convenient solutions for diffraction of these beams or even by purely Gaussian beams, by local canonical structures, are not available.

The accuracy of these representations of the reference pattern well off the beam axis is not essential because the field amplitudes are low and because the truncated Fourier transform representation of an aperture radiation pattern is itself an approximation, which is most accurate on the beam

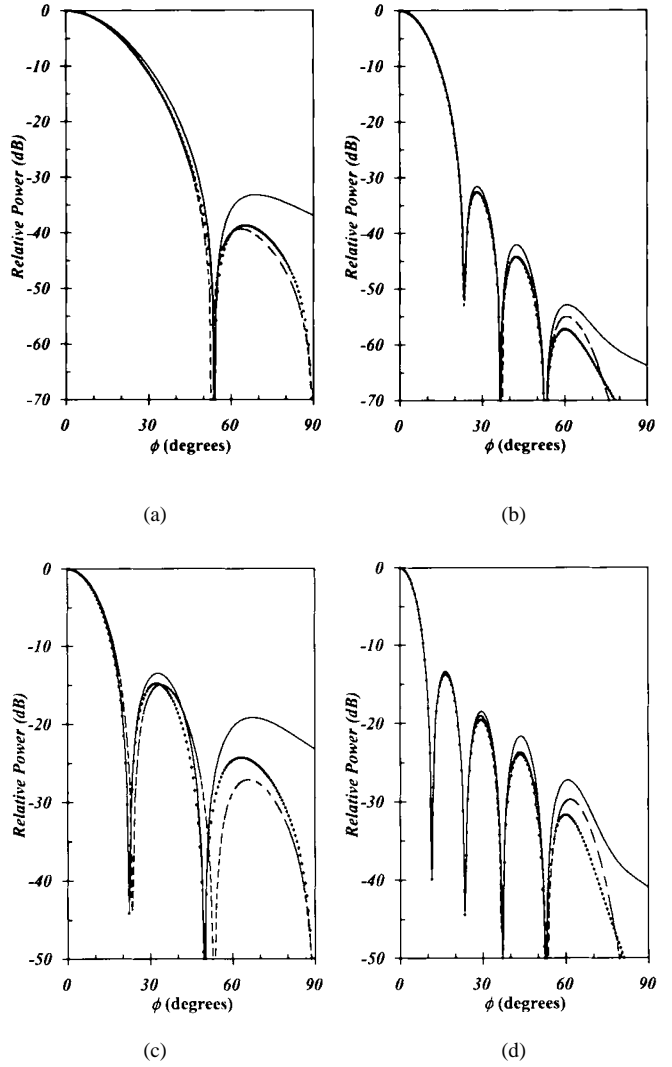


Fig. 2. The far-field patterns for cosine-squared and uniform aperture distributions. (a) Cosine-squared distribution $M = 2$, $N = 0$, $L_o = 2.5\lambda$, $L = \lambda/2$. (b) Cosine-squared distribution $M = 6$, $N = 0$, $L_o = 5\lambda$, $L = \lambda/2$. (c) Uniform distribution $M = 2$, $N = 0$, $L_o = 2.5\lambda$, $L = \lambda/2$. (d) Uniform distribution $M = 8$, $N = 0$, $L_o = 5\lambda$, $L = \lambda/2$. — complex line source solution —●—●— Gaussian beam solution - - - reference solution.

axis and progressively less accurate off it—an outcome of Kirchhoff diffraction theory.

In Fig. 2 the radiation patterns are at a distance from the aperture sufficiently large that all rays paths from the aperture plane to the field point are essentially parallel. When this assumption is removed and the radiation field in the Fresnel zone of the aperture is examined, it is found that the computation sequence associated with the beam series can be carried out not only in the far field, but also arbitrarily close to the aperture in the Fresnel region [1], [2]. Fig. 3 shows an example for a uniform distribution in an aperture of width $L_o = 5\lambda$. With the same number of complex line sources as the radiation far field calculation, it provides a good agreement with the approximate truncated Fresnel transform result over the main beam and first sidelobes. The Fresnel transform result

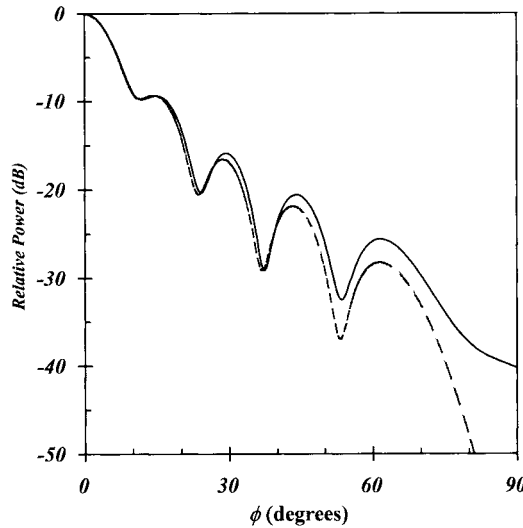


Fig. 3. The near field for a uniform aperture distribution. $M = 8, N = 0, L_o = 5\lambda, L = \lambda/2, r = L_o^2/2\lambda$. — complex source array solution, - - - Fresnel transform solution.

is based on including only first order near field effects through a quadratic phase term, e.g., [10, p. 32] and, like the truncated Fourier transform result, is progressively less accurate off the beam axis.

III. DIFFRACTION BY A HALF-PLANE

A. Analytical Expressions

The exact total far field for a local source uniform in the direction parallel to the edge and incident on a conducting half-plane can be obtained by an integration of the corresponding plane wave solution over all incident angles. Alternatively, it can be deduced more simply by reciprocity from the exact solution for plane wave diffraction by a half-plane, e.g., [10, p. 83]. This has been used with the CSP method in solving single-beam diffraction by a half-plane [7]. Now, we extend this with the Gabor series to solve half-plane diffraction by an aperture distribution, as indicated in Fig. 1(a).

The total far-field diffraction pattern (2) is represented by a superposition of the diffraction patterns of discrete elementary beams linearly shifted with respect to one another by distances L along the aperture plane and linearly phase shifted between neighboring beams. For the basis element $B_{m,n}(x, y)$ here, we use the solution for the total field at r, θ in cylindrical coordinates due to an electric line source parallel to and at $r_{o[m]}, \theta_{o[m]}$ from the edge with beam parameters b_n, β_n defined as above. Thus, we have (8), shown at the bottom of the page, where (r, θ) and $(r_{s[m,n]}, \theta_{s[m,n]})$ are the observation

position and complex source position in polar coordinates, and $F(w)$ is the complex Fresnel integral

$$F(w) = e^{-j\pi/4} \int_{we^{j\pi/4}}^{\infty} e^{-u^2} du = \frac{\sqrt{\pi}}{2} e^{-j\pi/4} \operatorname{erfc}(we^{j\pi/4}). \quad (9)$$

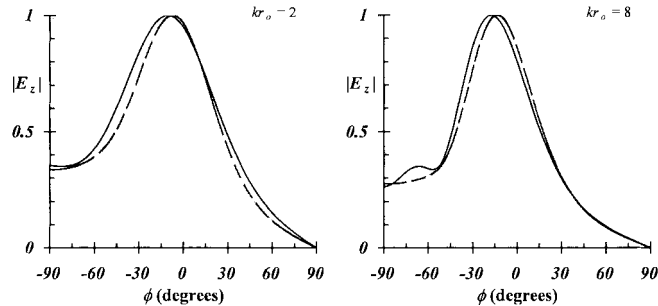
For computation of the elementary beam fields (8) it is necessary to have a Fresnel integral subroutine that can handle complex arguments. A computer subroutine for the complementary error function (erfc) with complex arguments is available.

B. Numerical Results

The solid curves in Fig. 4 represent the total field calculated from (2) with (8), for a distance above the half-plane kr_o ranging from 2 to 32 between the conducting edge and the center of the aperture plane with a cosine-squared aperture distribution. The angle of incidence θ_o of the center of the source with respect to the edge is $\pi/2$. The aperture size in wavelengths is $L_o = 2.5\lambda$. All the line source beams are spaced $L = \lambda/2$ apart and are normally directed at the half-plane ($\beta_n = 3\pi/2$). The relative weighting factors $A_{m,n}$ of each line source are calculated according to [2]. A narrower diffracted beam is obtained by moving the aperture plane further from the half-plane for then the beam illuminating the half-plane is narrower. For $kr_o = 32$ the pattern has more oscillations in the illuminated region ($-\pi/2 < \phi < 0$) due to interference between the direct wave from the line sources and a diffracted wave from the edge. In the shadow region ($0 < \phi < \pi/2$), the total far-field pattern decreases monotonically as ϕ increases and vanishes on the conductor. The field in the shadow region decreases more rapidly for larger kr_o because there is more blockage by the half-plane. Also shown for comparison are the results for incidence of a single line source beam with the same half-power beam width as the cosine-squared aperture far-field radiation pattern in isolation. Clearly, a single beam is a good approximation in this case, as might be expected for a cosine-squared aperture distribution.

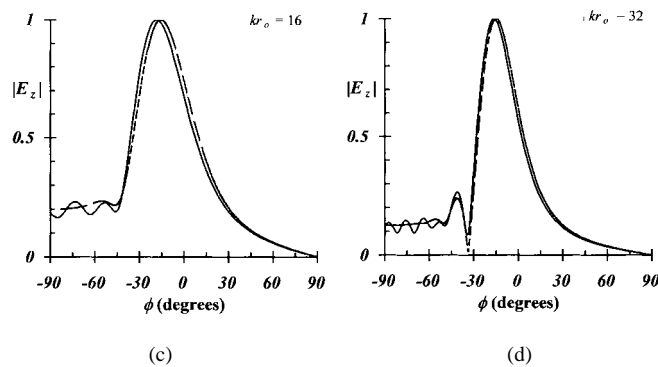
The total far field for an uniform aperture distribution has also been calculated from (2), with proper $A_{m,n}$ substitution and is shown in Fig. 5. Again, kr_o , the distance between the conducting edge and the aperture center ranges from 2 to 32. The major difference between Figs. 4 and 5 is the higher lobe levels in the illuminated region for the uniform aperture distribution due to interference between the larger direct wave and the diffracted wave from the edge. Also included are the results for single beam incidence. The half-power beamwidth of the single beam is the same as that of the uniform aperture far-field radiation pattern. Clearly, a single beam is not a good approximation in this case (as expected) since a single complex

$$B_{m,n}(r, \theta) = \frac{e^{-j(kr - \pi/4)}}{\sqrt{\pi kr}} \left\{ \begin{array}{l} e^{jkr_{s[m,n]} \cos(\theta - \theta_{s[m,n]})} F\left[-\sqrt{2kr_{s[m,n]}} \cos\left(\frac{\theta - \theta_{s[m,n]}}{2}\right)\right] \\ -e^{jkr_{s[m,n]} \cos(\theta + \theta_{s[m,n]})} F\left[-\sqrt{2kr_{s[m,n]}} \cos\left(\frac{\theta + \theta_{s[m,n]}}{2}\right)\right] \end{array} \right\} \quad (8)$$



(a)

(b)



(c)

(d)

Fig. 4. A comparison of normalized far-field diffraction patterns of a cosine-squared aperture distribution and a single CSP of the same beamwidth ($kb = 11.5$) at a distance ro from the edge of a perfectly conducting half-plane. $M = 2, N = 0, L_o = 2.5\lambda, \bar{L} = \lambda/2, \theta_o = \pi/2$. — cosine-squared — — — $kb = 11.5$.

line source beam cannot accurately represent the far field of an uniform aperture distribution.

In order to verify the accuracy and validity of the computer programs, the exact series solution for the total field due to a set of complex line sources diffracted by a conducting half-plane was programmed, i.e.,

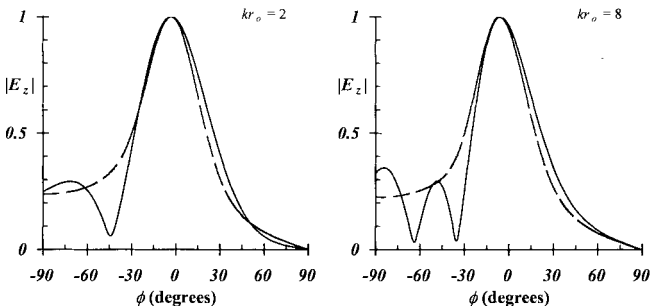
$$E_y = \sum_{m=-M}^M \sum_{n=-N}^N A_{m,n} \frac{e^{-jkr}}{\sqrt{kr}} \sum_{p=1}^{\infty} e^{jp\pi/2q} J_{p/q}(kr s_{[m,n]}) \cdot \sin\left(\frac{p\theta_{s[m,n]}}{q}\right) \sin\left(\frac{p\theta}{q}\right) \quad (10)$$

$J_k(z)$ is the Bessel function of the first kind of order k and here $q = 2$ for a half-plane. The $A_{m,n}$ are the same amplitude coefficients for the distribution calculated as in (2). It was found that twenty terms in (10) provides results essentially identical with those calculated from (2) for a cosine-squared distribution at $kr_o = 2$ in Fig. 4. This is an alternative formulation and capable of equal accuracy but it is much less efficient than using (8) for the basis functions, particularly for larger apertures and at larger ranges from the half-plane.

IV. DIFFRACTION BY A WIDE SLIT

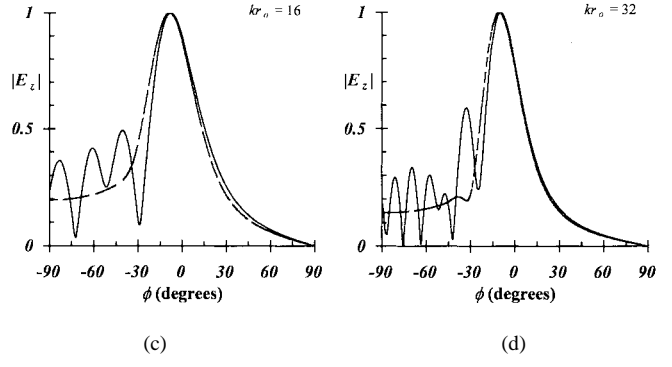
A. Analysis

A slit between two coplanar half-planes with parallel edges has been a traditional test of diffraction theories. By using the



(a)

(b)



(c)

(d)

Fig. 5. A comparison of normalized far-field diffraction patterns of a uniform aperture distribution and a single CSP of the same beamwidth ($kb = 22.84$) at a distance ro from the edge of a perfectly conducting half-plane. $M = 2, N = 0, L_o = 2.5\lambda, L = \lambda/2, \theta_o = \pi/2$. — cosine squared — — — $kb = 11.5$.

results for beam diffraction by a half-plane, we can solve the problem of beam diffraction by a wide slit in a conducting plane.

Fig. 1(b) shows an aperture field parallel to and at a height $y_o = L_o/2$ above the center of a slit in $y = 0, |x| \leq L_o/2$. The total noninteraction far field of the slit is the sum of the total far field of the half-plane on the right side and that on the left side less an incident field. The total far field of the half-plane on the right side is given by replacing r_1, θ_1 with r, θ and $r_{s1[m,n]}, \theta_{s1[m,n]}$ with $r_{s[m,n]}, \theta_{s[m,n]}$ in the elementary beam field $B_{m,n}(r, \theta)$ (8). Similarly, the total far field of the half-plane on the left side is given by replacing r_2, θ_2 with r, θ and $r_{s2[m,n]}, \theta_{s2[m,n]}$ with $r_{s[m,n]}, \theta_{s[m,n]}$ in the elementary beam field $B_{m,n}(r, \theta)$. In the far field ($r \gg L_o$), the singly diffracted far fields of the slit can be calculated by (2) with (11), shown at the bottom of the next page.

B. Numerical Results

The diffraction patterns of Fig. 6(a) and (b) are calculated for an inphase cosine-squared aperture distribution in apertures of width $L_o = 5\lambda$ and 9λ , respectively. The apertures are parallel to and at heights $y_o = L_o/2$ and $10L_o$ above a slit with the same width as the aperture. The solid and dotted curves are for only noninteraction diffraction fields calculated from complex line sources located along the aperture plane. For Fig. 6(a) they have the same weighting factors as in Fig. 2(b). For comparison, the far-field patterns for a cosine-squared

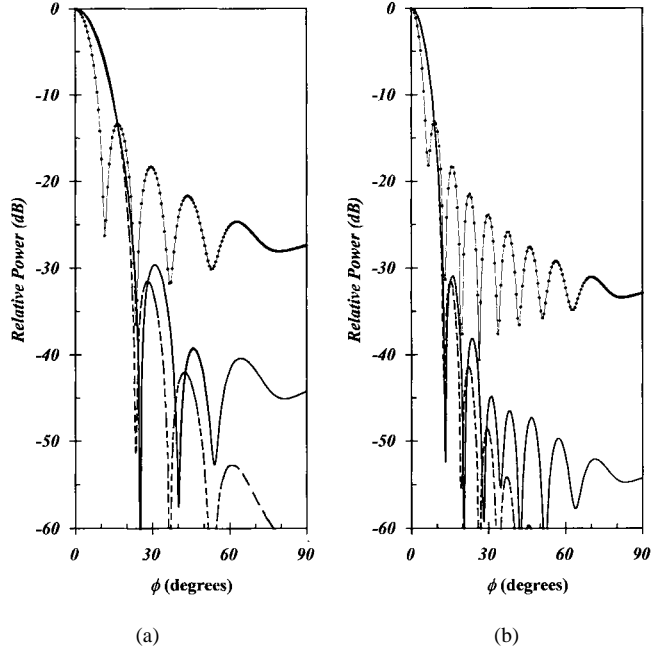


Fig. 6. Normalized far-field diffraction patterns of a slit of width L_o excited by a cosine-squared distribution at y_o behind the center of the slit. (a) $M = 6, N = 0, L_o = 5\lambda, L = \lambda/2$. (b) $M = 9, 1N = 0, L_o = 9\lambda, L = \lambda/2$. — aperture at $y_o = L_o/2$ above the slit. —●—●—●— aperture at $y_o = 10L_o$ above the slit. —— aperture alone.

distribution with the slit absent are also included as dashed curves.

Figs. 6 show that with the radiating aperture close to the slit, the far-field diffraction patterns have the same number of sidelobes but moderately higher sidelobe levels than the total far field patterns with the slit absent. With the aperture further away at $y_o = 10L_o$ the resulting patterns are more profoundly altered with narrower main beams and more and much higher sidelobe levels. The slit is now essentially uniformly illuminated so the resulting diffraction patterns essentially those for plane wave incidence on the slit.

The last example is a comparison of the normalized far-field diffraction patterns of a slit of width L_o excited by a cosine-squared distribution with a single complex line source with the same

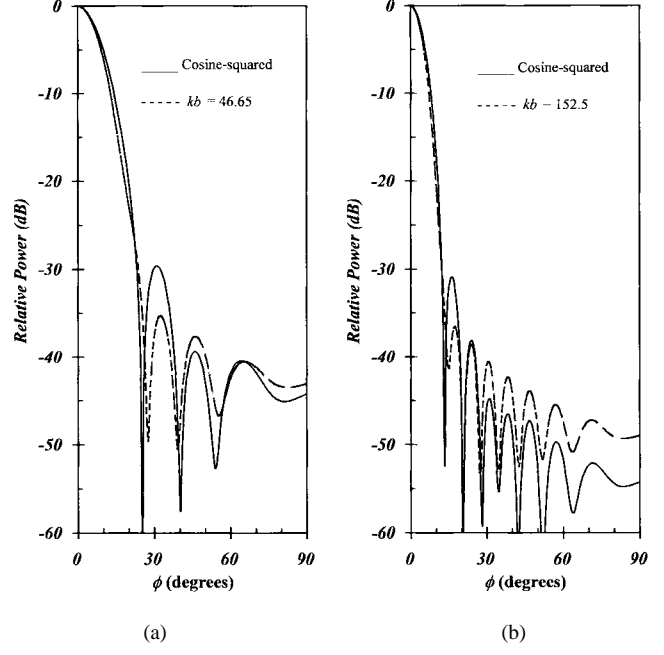


Fig. 7. Normalized far-field diffraction patterns of a slit of width L_o excited by a cosine-squared distribution and a single complex line source with beam directivity kb at $y_o = L_o/2$ behind the center of the slit. (a) $M = 6, N = 0, L_o = 5\lambda, L = \lambda/2$. (b) $M = 9, 1N = 0, L_o = 9\lambda, L = \lambda/2$.

half-power beam width in the far-field radiation pattern. In Fig. 7, the solid curves are the result for an array of complex line sources simulating a cosine-squared aperture distribution and the dashed curve represents a single line source with the same half-power beam width. For both cases ($L_o = 5\lambda, 9\lambda$), the single line source solution shows lower sidelobes level near the axis and higher sidelobe levels far away from the axis than the beam series computation. Here the local obstacle (the slit) is very close to the aperture plane ($y_o = L_o/2$). This shows that while the cosine-squared distribution and paraxial complex line source (Gaussian beam) may have similar beam shapes, a single complex line source can not accurately predict the diffraction pattern of an extended source at this range.

The calculations described above are accurate only for slits sufficiently wide that interaction between them is negligible.

$$B_{m,n} = \frac{e^{-j(kr - \pi/4)}}{\sqrt{\pi kr}} \left\{ \begin{array}{l} -e^{jk(L_o/2) \sin \phi} \left[e^{jkr_{s1[m,n]} \sin(\phi - \theta_{s1[m,n]})} F\left(\sqrt{2kr_{s1[m,n]}} \cos\left(\frac{3\pi}{2} + \phi - \theta_{s1[m,n]}\right)\right) \right. \\ \quad \left. + e^{jkr_{s1[m,n]} \sin(\phi + \theta_{s1[m,n]})} F\left(-\sqrt{2kr_{s1[m,n]}} \cos\left(\frac{3\pi}{2} + \phi + \theta_{s1[m,n]}\right)\right) \right] \\ + e^{jk(L_o/2) \sin \phi} \left[e^{-jkr_{s2[m,n]} \sin(\phi - \theta_{s2[m,n]})} F\left(-\sqrt{2kr_{s2[m,n]}} \cos\left(\frac{\pi}{2} + \phi - \theta_{s2[m,n]}\right)\right) \right. \\ \quad \left. - e^{-jkr_{s2[m,n]} \sin(\phi + \theta_{s2[m,n]})} F\left(-\sqrt{2kr_{s2[m,n]}} \cos\left(\frac{\pi}{2} + \phi + \theta_{s2[m,n]}\right)\right) \right] \end{array} \right\} \quad (11)$$

For more accurate results, inclusion of interaction between the edges is necessary. The field singly diffracted from each edge of the conducting half-plane in the direction of the opposite edge of the other conducting half-plane is replaced by the field of a line source of equal amplitude located at the edge from which the singly diffracted field emanated. This procedure can be used to improve the accuracy by the including first-order interaction field. However, the edge diffraction fields are not omnidirectional as assumed for a line source, so the results are not made more accurate by repeating the above procedure. Since higher order interaction is weak in the examples studied above, as shown in [7], it is sufficient to include only noninteraction fields here.

Only radiating beams from the aperture are included in calculating Figs. 6 and 7. If the aperture-slit separation is small in wavelengths, diffraction by the evanescent fields of the aperture, represented by beams at complex angles, may require inclusion. If the slit width is large compared to the aperture width and aperture-slit separation, additional tilted or aligned beams at smaller separations than a half wavelength may be required to improve accuracy at large angles off the aperture pattern axis.

V. CONCLUSIONS

The CSP technique is known already as a very efficient means of extending point or line source diffraction solutions to beam solutions. Gaussian beams in a Gabor series have also been established as a complete representation of the fields of a radiating aperture [1], [2] and it was indicated [1] that the two techniques could be effectively combined. Here this is done for diffraction by half-planes and slits in the presence of 2-D radiating apertures. Only symmetrical aperture distributions were chosen here as the simplest and most common examples, but the method may be extended to arbitrary-shaped aperture distributions on nonplanar as well as planar surfaces.

An efficient solution has a minimum number of beams. This depends on the situation under consideration and warrants a demonstration of the accuracy of the beam arrangement used to represent the aperture field in isolation. Previous numerical investigations [1], [2] provided a useful guide but generally have more beams than were found to be needed here. Moreover, Gaussian beams rather than complex source beams were used, so it is necessary demonstrate the differences introduced by using the latter. These may be significant with small apertures represented by few sources and occur mainly at wide angles off the pattern main beam axis. The advantage of using CSP beams is not only that they represent an exact solution to the wave equation, but also that they allow the use of rigorous and convenient elementary beam diffraction solutions. For the half-plane this solution is exact and rather simple.

The beam amplitudes in (1) may be determined directly from the aperture distribution profile if the beams are very closely spaced [1]. Closer beam spacings imply broader beams and with beam spacings of say, a tenth of a wavelength or less, omnidirectional line sources should suffice. A simpler asymptotic solution than this would then be a superposition

of many real line source solutions with amplitudes according to the distribution profile and regular use of UTD. It would not be efficient however, because of the larger number of line source solutions to be evaluated and included. With line source solutions spaced half a wavelength (as in the numerical examples here) the accuracy deteriorates, particularly off the main lobe of the aperture radiation pattern and off the main lobe of the diffraction pattern in the examples of Figs. 4 and 5. The accuracy of the results in Figs. 6 and 7 may be less affected if the slit edges lie well within the main lobe of the aperture pattern. In general, however, the beam series representation permits the use of fewer more widely separated source solutions and this is its advantage over a simple asymptotic solution consisting of many more closely spaced line source solutions. Beam spacings of a half wavelength seem to minimize the number of beams required, at least for smaller apertures, as larger spacings require both aligned and tilted beams [2]. Of course, the beam amplitudes, once determined, apply for any scatterer at almost any range.

It is useful to confirm here that a single beam is a good approximation for half-plane diffraction if the aperture width is not large and the distribution symmetrically tapered. Two-dimensional noninteraction fields for aperture diffraction by a wide slit were calculated also. Then even for apertures not large and with tapered distributions, when the local object is close to the aperture plane, a single beam source does not represent the diffraction pattern accurately.

Usually, shadow and reflection boundaries must be located in applying the geometrical theory of diffraction. Although the location of shadow and reflection boundaries is no difficulty for the CSP method, the shadow and reflection boundary locations are not needed here because a uniform total field solution is used.

An array of complex sources is a powerful technique for calculating the effects of local obstacles on antenna patterns. It is not just that this method is convenient in these simple examples. It also opens up a range of problems which can now be treated rigorously. This procedure has already been applied to other canonical structures and these results will be reported.

REFERENCES

- [1] J. J. Maciel and L. B. Felsen, "Systematic study of fields due to extended apertures by Gaussian beam discretization," *IEEE Trans. Antennas Propagat.*, vol. 37, pp. 884-892, July 1989.
- [2] P. D. Einziger, S. Raz, and M. Shapira, "Gabor representation and aperture theory," *J. Opt. Soc. Amer.*, vol. 3, pt. A, no. 4, pp. 508-522, 1986.
- [3] M. J. Bastiaans, "A sampling theorem for the complex spectrogram and Gabor's expansion of a signal in Gaussian elementary signals," *Opt. Eng.*, vol. 20, p. 594, 1981.
- [4] L. B. Felsen, "Geometrical theory of diffraction, evanescent waves, complex rays and Gaussian beams," *Geophys. J. R. Astron. Soc.*, pp. 77-88, 1984.
- [5] G. A. Deschamps, "Gaussian beam as a bundle of complex rays," *Electron. Lett.*, vol. 7, pp. 684-685, 1971.
- [6] L. B. Felsen, "Evanescent waves," *J. Opt. Soc. Am. A*, vol. 66, no. 8, pp. 751-760, 1962.
- [7] G. A. Suedan and E. V. Jull, "Two-dimensional beam diffraction by a half-plane and wide slit," *IEEE Trans. Antennas Propagat.*, vol. AP-35, pp. 1077-1083, Sept. 1987.

- [8] G. A. Sordan and E. V. Jull, "Beam diffraction by half-planes and wedges: Uniform and asymptotic solutions," *J. Electromagn. Waves Applcat.*, vol. 3, no. 1, pp. 17-26, 1989.
- [9] A. J. E. M. Jansen, "Gabor representation of generalized function," *J. Math. Anal. Appl.*, vol. 83, pp. 377-394, 1981.
- [10] E. V. Jull, "Aperture antennas and diffraction theory," *Institute of Electrical Engineers Electromagnetic Wave Series*. Stevenage, U.K.: Peter Peregrinus, 1981, vol. 10.

Hong D. Cheung was born in Taiwan. He received the B.Sc. degree in physics from York University, Ontario, Canada, in 1994, and the Ph.D. degree in electrical and computer engineering from the University of British Columbia, Canada, in 1999.

He currently works in the Electrical and Computer Engineering Department of the University of British Columbia as a Research Assistant. His research interests include the complex source point method and high-frequency wave propagation and diffraction theory.

Edward V. Jull (LF'98) was born in Calgary, Canada. He received the B.Sc. degree in engineering physics from Queen's University, Kingston, Canada, in 1956, and the Ph.D. (electrical engineering) and the D.Sc. (Eng.) degrees in from University College, London, U.K., in 1960 and 1979, respectively.

He was with the Division of Radio and Electrical Engineering of the National Research Council, Ottawa, Canada, from 1961 to 1972. He is now a Professor in the Department of Electrical and Computer Engineering, University of British Columbia, Vancouver, Canada. His research interests include aperture antennas and diffraction theory.

Dr. Jull is a Past President of the International Union of Radio Science (URSI) (1990-1993).